Supporting Information for ***Journal of Materials Chemistry A***

Engineering the Metal Organic Framework Derived 3D Nanostructures for High Performance Hybrid Supercapacitor

Rutao Wang[a,b], Dongdong Jin[a], Yabin Zhang[a], Shijie Wang[a], Junwei Lang[b], Xingbin Yan[b]*, Li Zhang[a]*

[a] Department of Mechanical and Automation Engineering, The Chinese University of Hong Kong, Shatin NT, Hong Kong SAR, China

[b] Laboratory of Clean Energy Chemistry and Materials, State Key Laboratory of Solid Lubrication, Lanzhou Institute of Chemical Physics, Chinese Academy of Sciences, Lanzhou, 730000, P.R. China

*E-mail address: lizhang@mae.cuhk.edu.hk & xbyan@licp.cas.cn

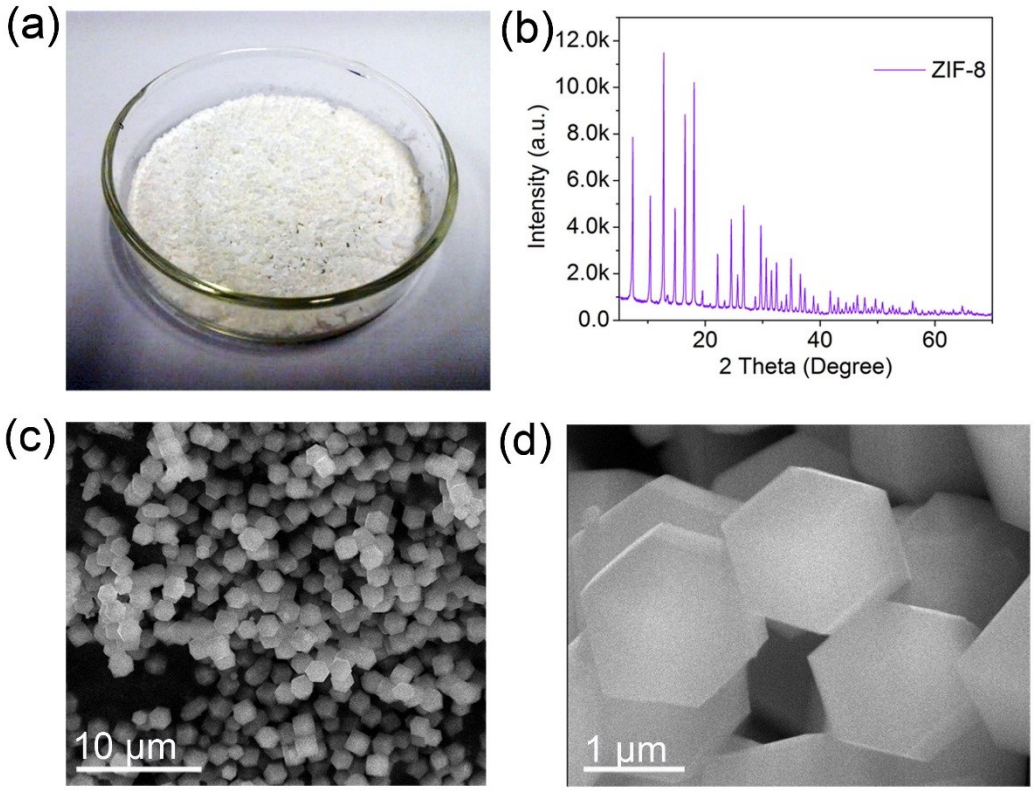

Fig. S1 (a) Optical image of ZIF-8, (b) XRD pattern of ZIF-8, (c) and (d) SEM images of ZIF-8 sample.

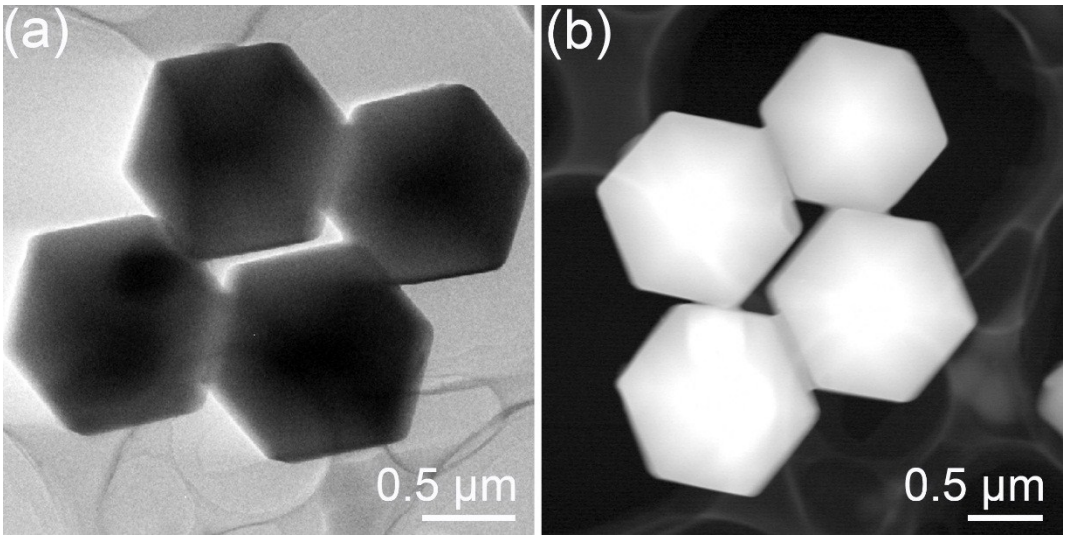

Fig. S2 (a) TEM image and (b) the corresponding ADF-TEM image of ZIF-8-800 sample.

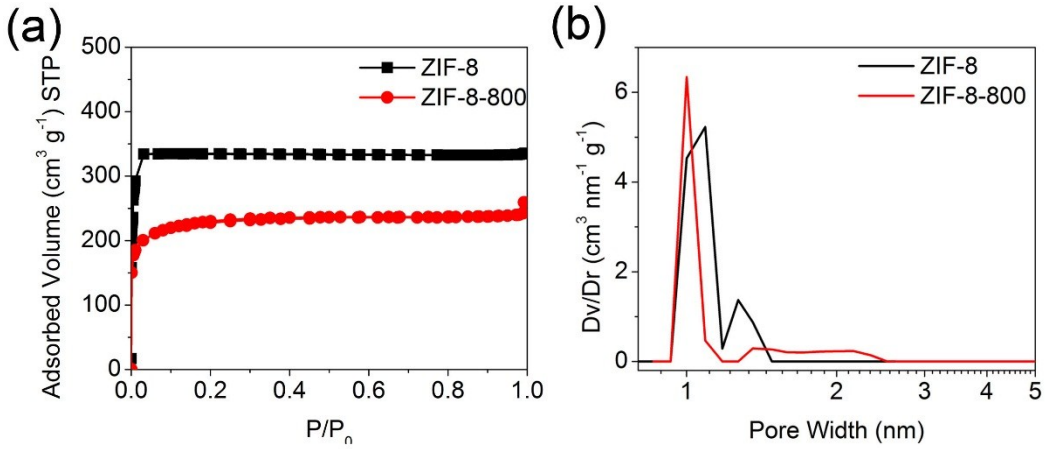

Fig. S3 (a) Nitrogen adsorption-desorption isotherms and (b) pore-size distributions of ZIF-8 and ZIF-8-800 samples.

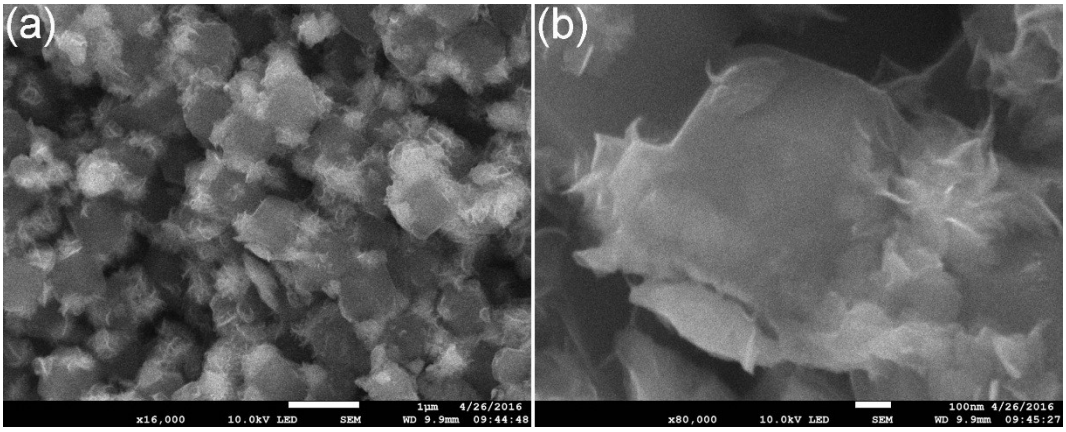

Fig. S4 SEM images of MoS_2-ZIF sample without the addition of glucose in the hydrothermal procedure.

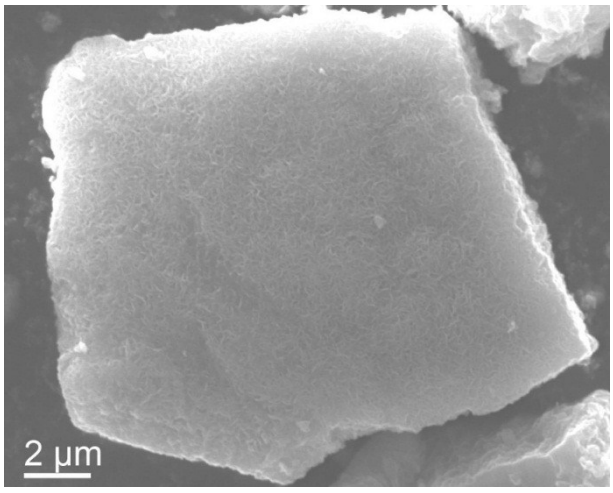

Fig. S5 SEM image of pure MoS_2 sample.

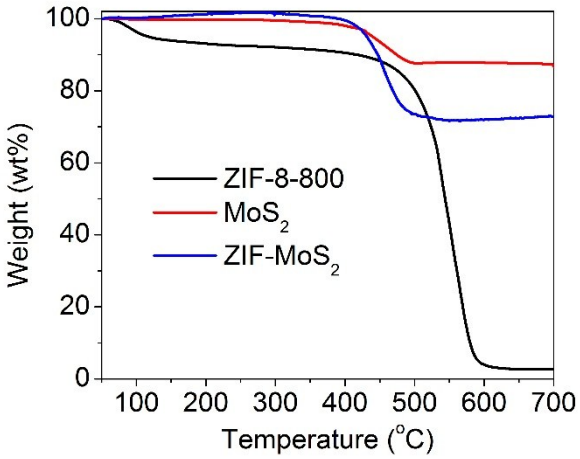

Fig. S6 TGA curves of ZIF-8, ZIF-8-800, and MoS_2-ZIF samples.

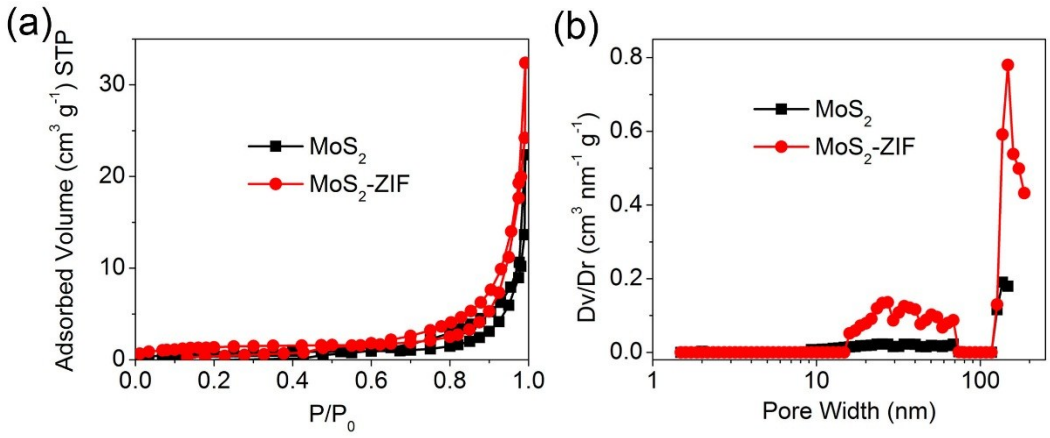

Fig. S7 (a) Nitrogen adsorption-desorption isotherms and (b) the corresponding pore-size distributions of MoS_2 and MoS_2-ZIF samples.

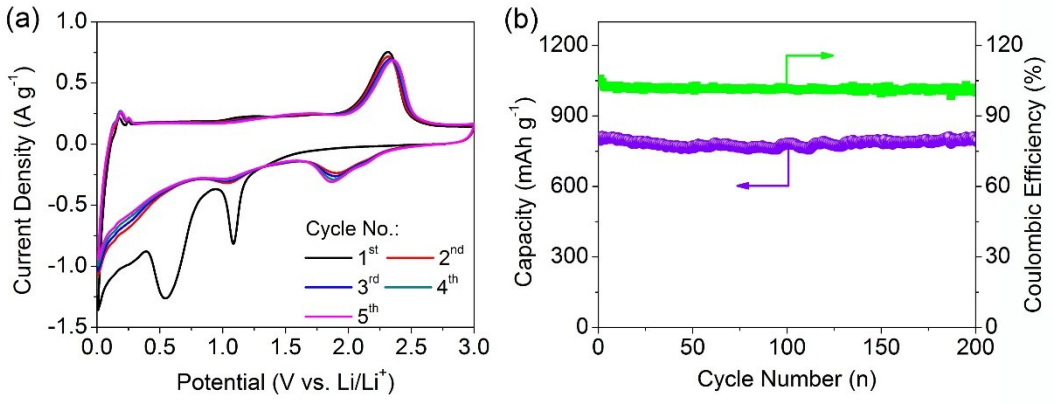

Fig. S8 (a) CV curves of MoS_2-ZIF electrode at a potential scan rate of 0.2 mV s^{-1}, (b) cycling performance of MoS_2-ZIF sample at a current density of 1 A g^{-1}.

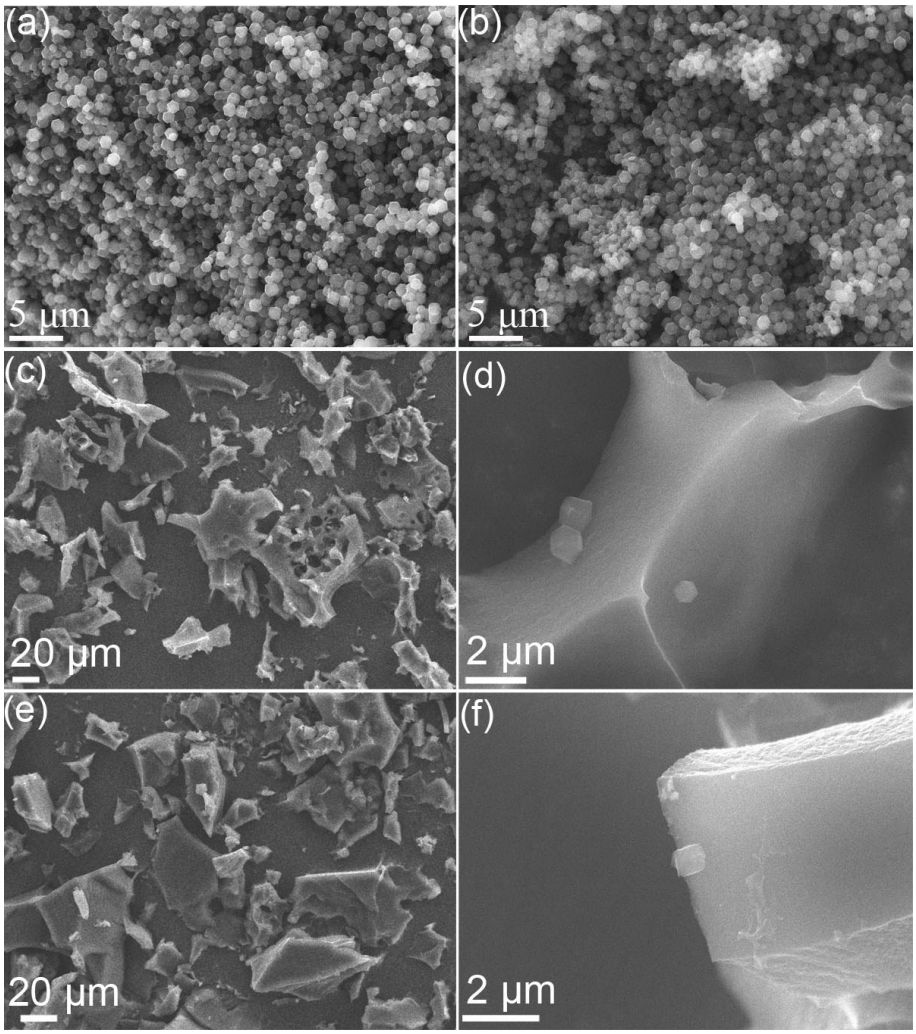

Fig. S9 SEM images of ZDPC samples: (a) ZDPC-1, (b) ZDPC-2, (d) and (e) ZDPC-3, (f) and (g) ZDPC-4.

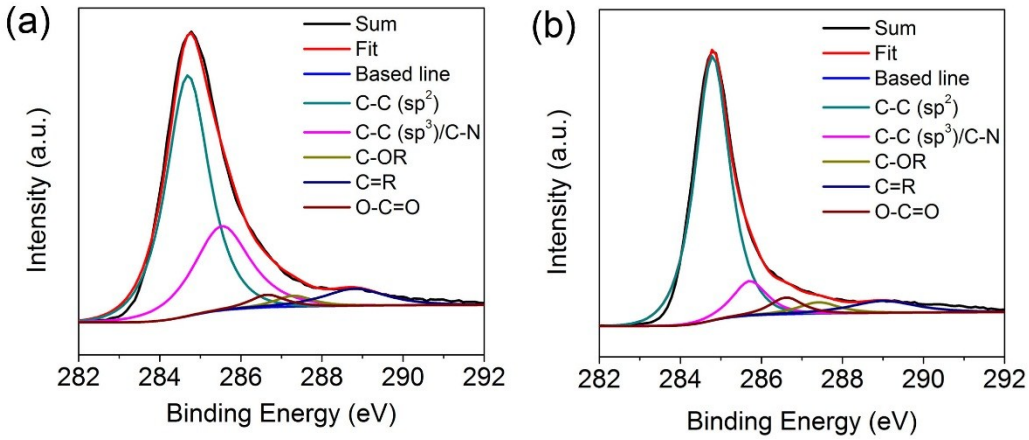

Fig. S10 High-resolution C1s XPS spectra of (a) ZIF-8-800 and (b) ZDPC-2 samples.

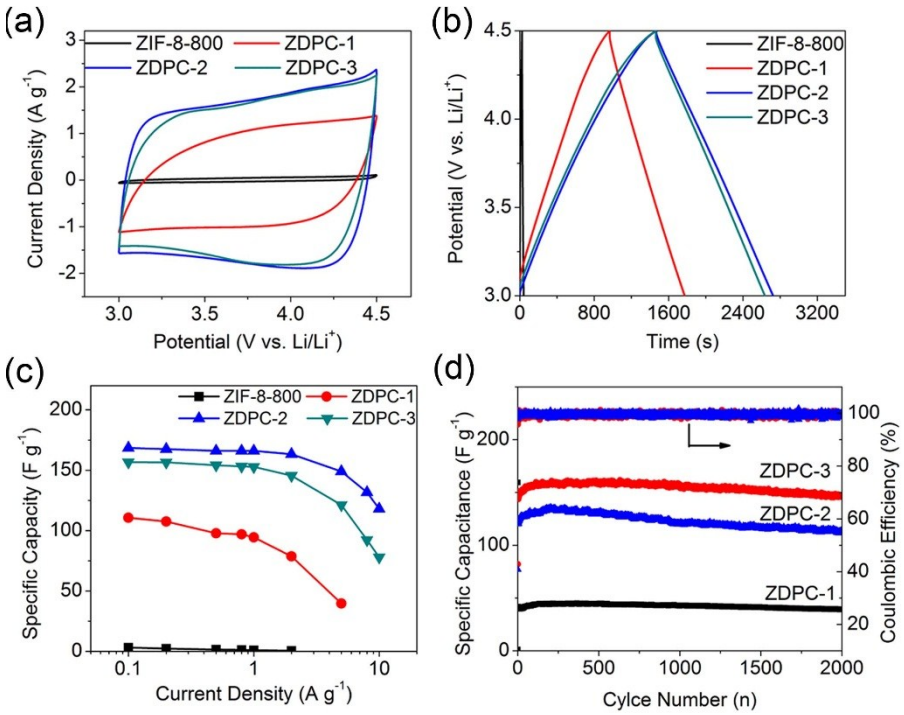

Fig. S11 (a) Typical CVs of ZDPC samples and ZIF-8-800 at a scan rate of 10 mV s^{-1} with a potential range of 3-4.5 V (vs. Li/Li^+). (b) Charging/discharging curves of ZDPC samples and ZIF-8-800 at the current densities at 0.2 A g^{-1} with a potential range of 3-4.5 V (vs. Li/Li^+). (c) Rate capability of ZIF-8-800 and ZDPC electrodes at various current densities ranging from 0.1 to 10 A g^{-1} with a potential range of 3-4.5 V (vs. Li/Li^+). (d) Cycling performance of ZDPC samples at current density of 5 A g^{-1} and the corresponding columbic efficiency of ~100% with a potential range of 3-4.5 V (vs. Li/Li^+).

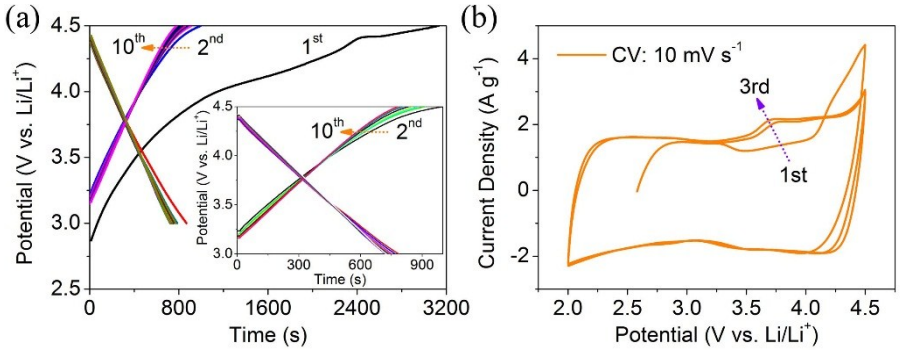

Fig. S12 (a) Initial charge/discharge curves with a current density of 0.34 A g^{-1} and (b) CV curves with a sweep rate of 10 mV s^{-1} for ZDPC-2 electrode. A polarization can be observed in first charge/discharge curve and in first CV curve as the potential is larger than 4.1 V, but it can be largely reduced in the second cycles. The polarization for ZDPC-2 may be related to side effects caused by residual water and impurities, surface heteroatoms, and/or the electrochemical activation process. Both the charging and discharge process curves in the following cycles have notable slopes, which indicate a reversible, non-Faradaic reaction such as adsorption/desorption of PF_6^- anions. No significant change in size or shape is observed in the following third CV curve as compared with second CV cycle, indicating a good reversibility.

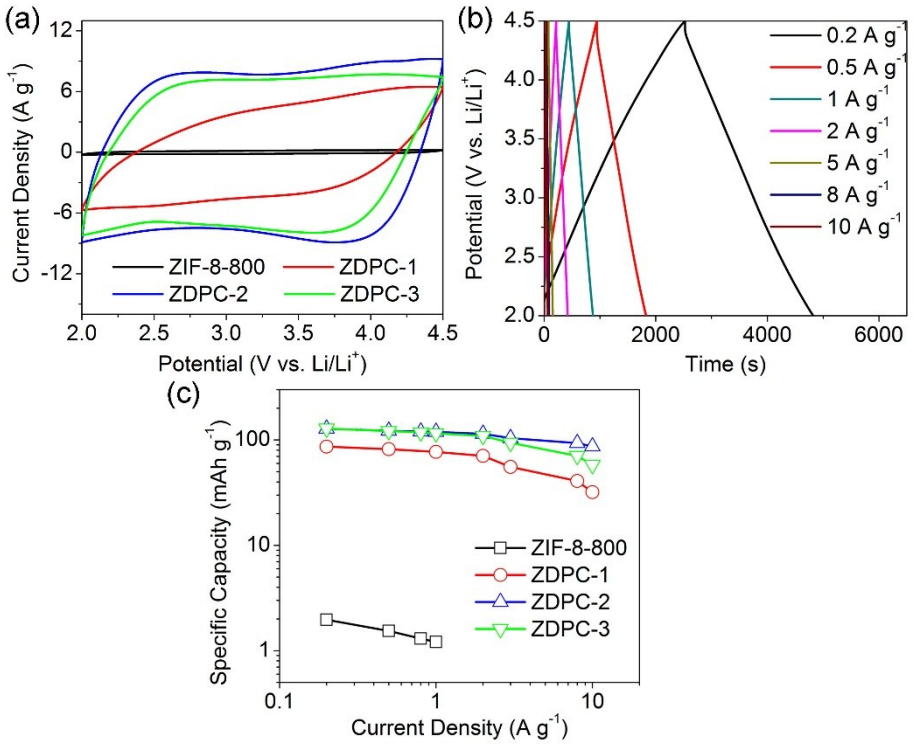

Fig. S13 The electrochemical performance of ZIF-8-800 and ZDPC samples in Li-half cell: (a) CV curves at a sweep rate of 50 mV s^{-1}, (b) charge/discharge cuvees at a wide current range from 0.2 to 10 A g^{-1} for ZDPC-2 sample, (c) rate capability of pure ZIF-8-800 and ZDPC electrodes.

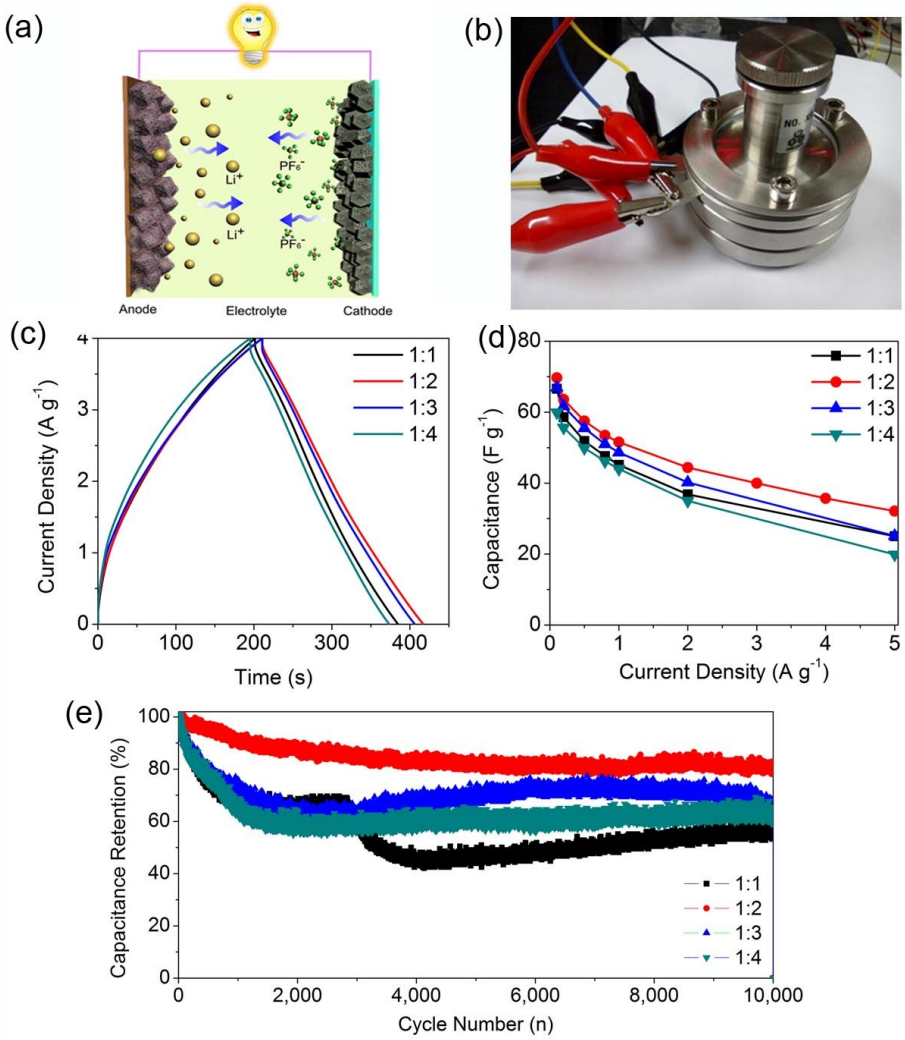

Fig. S14 (a) Schematic illustration of this MoS_2-ZIF//ZDPC hybrid configuration at the discharging state. (b) Optical image of a commercial three electrode system (EQ-3ESTC, Heifei Kejing Materials Technology. Co., LTD, China) used to analysis the potential window (*vs.* Li/Li^+) of positive and negative electrodes in this hybrid LIC during charging/discharging process. Electrochemical characterizations of MoS_2-ZIF//ZDPC hybrid LICs with the different anode/cathode mass ratios: (c) galvanostatic charge/discharge curves at a different current density of 1 A g^{-1}, (d) specific capacitance values calculated from galvanostatic charge/discharge curves under different current densities, and (e) cycle stability for 10,000 cycles at a current density of 2 A g^{-1}.

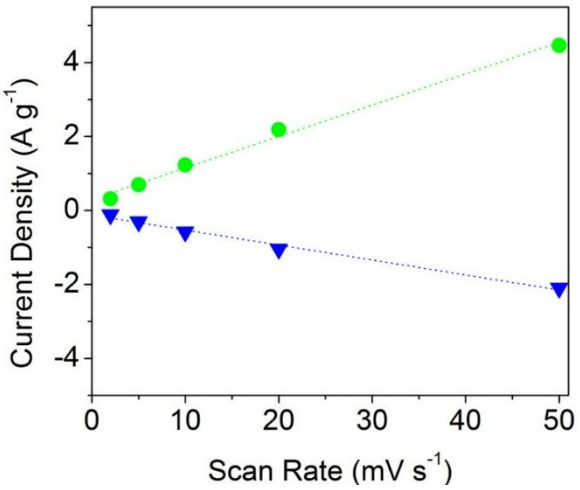

Fig. S15 The variation of charge and discharge peak currents with the CV scan rates of MoS_2-ZIF//ZDPC hybrid LIC.

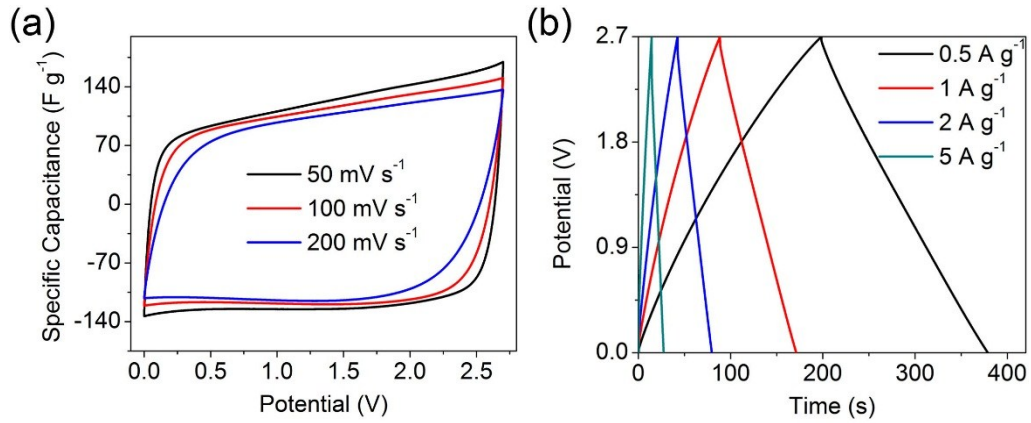

Fig. S16 (a) Typical CVs of symmetric ZDPC//ZDPC (using ZDPC-2 as the active materials) symmetric supercapacitor at various scan rates, and (b) charging/discharging curves of symmetric ZDPC//ZDPC symmetric supercapacitor at the current densities ranging from 0.5 to 5 A g^{-1}.

Table S1 Carbon structure and surface chemistry properties of ZIF-8-800 and ZDPC-*x* samples.

Sample	Carbon structure					Surface chemistry (XPS)		
	d_{002} (nm)	*R* (nm)	*La* (nm)	*Lc* (nm)	I_G/I_D[a]	C (wt%)	N(wt%)	O(wt%)
ZIF-8-800	0.354	1.30	10.59	1.1	0.551	76.03	15.83	8.14
ZDPC-1	0.340	0.45	9.42	1.1	0.486	86.89	6.01	7.09
ZDPC-2	0.340	0.43	9.42	1.0	0.488	91.97	1.31	6.72
ZDPC-3	0.345	0.46	8.84	1.0	0.463	92.9	0.87	6.24

[a] I_D and I_G are the integrated intensities of D- and G- band for carbon material.

Table S2 Summary of pore-structure properties of ZIF-8, ZIF-8-800, and ZDPC-*x* samples

Samples	S_{BET} (m^2 g^{-1})	APW[a] (nm)	Pore Volume (cm^3 g^{-1})	Micropore %	Mesopore %
ZIF-8	1081	1.91	0.52	100	0
ZIF-8-800	784.3	1.89	0.37	93.99	8.01
ZDPC-1	2653.8	2.23	1.45	52.92	47.08
ZDPC-2	3680.6	2.11	1.94	40.14	59.86
ZDPC-3	3280.1	3.72	3.02	12.47	87.53

[a] APW means average pore width.

Table S3 Summary of electrochemical characteristics of reported LICs and our MoS_2-ZIF//ZDPC LIC.

LIC type	Positive type and Capacity	Working Potential (V)	Maximum Energy Density (Wh kg^{-1})	Maximum Power Density (W kg^{-1})	Cycle Number (n)	Cycle Stability (%)	References
MnO-graphene//graphene	N-doped Graphene (40-62 mAh g^{-1})	1-4	127	25,000	3,000	76	S1
3D MnO/GNS//GNS	N-doped graphene (70 mAh g^{-1})	1-4	184	15,000	5,000	76	S2
Fe_3O_4-graphene//AC	Sucrose derived AC (Not provided)	1-4	204	5,000	1,000	70	S3
TiN// N-doped AC	Polyaniline derived AC (40-80 mAh g^{-1})	0-4.5	101.5	67,500	5,000	82	S4
graphene//graphene	Graphene (Not provided)	0-4.2	180	20,000	1,000	90	S5
Si/C//N-doped AC	N-doped AC (80-120 mAh g^{-1})*	2-4.5	230	30,127	8,000	76.3	S6
$TiNb_2O_7$@carbon// CF	CF (80 mAh g^{-1})	2.8-4.2	99.58	5,464	1,500	77	S7
commercial AC/$LiNi_{0.5}Mn_{1.5}O_4$	Commercial AC (58 mAh g^{-1})	1.5-3.3	19	3,500	3,000	81	S8
B-Si/SiO_2/C//PSC	PSC microspheres (65 mAh g^{-1})*	2-4.5	128	9,704	6,000	70	S9
m-Nb_2O_5/C//MSP-	Commercial AC (68 mA g^{-1})	1-3.5	63	16,528	1,000	100	S10

20							
V_2O_5/RGO//RGO	Graphene (Not provided)	0-2.5	13.3	625	8,000	100	S11
RGO//RGO	Graphene (Not provided)	1.5-4.5	160	100,000	1,000	95	S12
LTO-graphene// AC	Sucrose derived AC (27-40 mAh g^{-1})	0-3	94	3,000	500	87	S13
$H_2Ti_6O_{13}$//CMK-3	CMK-3 (Not provided)	1-3.5	90	11,000	1,000	80	S14
VN-RGO// AC	Polyanline derived AC (52-79 mAh g^{-1})	0-4	162	10,000	1,000	83	S15
NbN-RGO// AC	Commercial AC (55 mAh g^{-1})	2-4	122.7	2,000	1,000	81.7	S16
T-Nb_2O_5/graphene// AC	Commercial AC (Not provided)	0.5-3	47	18,000	2,000	93	S17
Si/C//eAC-900	Biomass derive AC (40-129 mAh g^{-1})*	2-4.5	258	29,893	15,000	79.2	S18
Biomass carbon//AC	PJ-AC (40 mAh g^{-1})	2-4	162.3	4,500	7,000	79	S19
MoS_2-RGO//AC	Polyaniline derived AC (97.9 mAh g^{-1})*	0-4	156	8,314	1,000	78	S20
$Li_4Ti_5O_{12}$//MOF-DC	MOF-Carbon (66 mAh g^{-1})	1-3	65	10,000	10,000	82	S21
SnO_2-C//AC	Commercial AC (Not provided)	0.5-4	110	2,960	2,000	80	S22
Ti_2C(Mxene)//YP17	Commercial AC (55 mAh g^{-1})	1-3.5	50	19,000	1,000	85	S23
TiO_2-Graphene//AC	Commercial AC (55 mAh g^{-1})	1-3	42	8,000	7,000	100	S24
Graphite//AC	Commercial AC	1.5-4.5	103	10,000	10,000	85	S25
Prosopis juliflora derived carbon//AC	Biomass derived AC (100 mAh g^{-1})*	2-4	163	4,500	7,000	79	S26
Graphite//a-MEGO	-	2-4	147.8	-	-	-	S27
MoS_2-ZIF//ZDPC	**MOF derived AC (41.2-71.2 mAh g^{-1}), (86.7-127.2 mAh g^{-1})***	**0-4**	**155**	**20,000**	**10,000**	**81**	**This work**

*-Working potential 2-4 V (vs. Li/Li^+)

References

S1 M. Yang, Y. Zhong, J. Ren, X. Zhou, J. Wei and Zhen Zhou, *Adv. Energy Mater.*, 2015, **5**, 1500550.

S2 H. Wang, Z. Xu, Z. Li, K. Cui, J. Ding, A. Kohandehghan, X. Tan, B. Zahiri, B. C. Olsen, C. M. B. Holt and David Mitlin, *Nano Lett.*, 2014, **14**, 1987–1994.

S3 F. Zhang, T. Zhang, X. Yang, L. Zhang, K. Leng, Y. Huang and Y. Chen, *Energy Environ. Sci.*, 2013, **6**, 1623-1632.

S4 H. Wang, Y. Zhang, H. Ang, Y. Zhang, H. T. Tan, Y. Zhang, Y. Guo, J. B. Franklin, X. L. Wu, M. Srinivasan, H. J. Fan and Q. Yan, *Adv. Funct. Mater.*, 2016, **26**, 3082-3093.

S5 X. –Y. Shan, Y. Wang, D. –W. Wang, F. Li and H. -M. Cheng, *Adv. Energy Mater.*, 2016, **6**, 1502064.

S6 B. Li, F. Dai, Q. Xiao, L. Yang, J. Shen, C. Zhan and M. Cai, *Energy Environ. Sci.*, 2016, **9**, 102-106.

S7 X. Wang and G. Shen, *Nano Energy*, 2015, **15**, 104-115.

S8 N. Arun, A. Jain, V. Aravindan, S. Jayaraman, W. C. Ling, M. P. Srinivasan and S. Madhavi, *Nano Energy*, 2015, **12**, 69-75.

S9 R. Yi, S. Chen, J. Song, M. L. Gordin, A. Manivannan and D. Wang, *Adv. Funct. Mater.,* 2014, **24**, 7433-7439.

S10 E. Lim, C. Jo, H. Kim, M. -H. Kim, Y. Mun, J. Chun, Y. Ye, J. Hwang, K. -S. Ha, K. C. Roh, K. Kang, S. Yoon and J. Lee, *ACS Nano*, 2015, **9**, 7497-7505.

S11 C. Y. Foo, A. Sumboja, D. J. H. Tan, J. Wang and P. S. Lee, *Adv. Energy Mater.*, 2014, **4**, 1400236.

S12 B. Z. Jang, C. Liu, D. Neff, Z. Yu, M. C. Wang, W. Xiong and A. Zhamu, *Nano Lett.*, 2011, **11**, 3785–3791.

S13 K. Leng, F. Zhang, L. Zhang, T. Zhang, Y. Wu, Y. Lu, Y. Huang and Y. Chen, *Nano Res.*, 2013, **6**, 581-592.

S14 Y. Wang, Z. Hong, M. Wei and Y. Xia, *Adv. Funct. Mater.*, 2012, **22**, 5185–5193.

S15 R. Wang, J. Lang, P. Zhang, Z. Lin and X. Yan, *Adv. Funct. Mater.*, 2015, **25**, 2270-2278.

S16 M. Liu, L. Zhang, P. Han, X. Han, H. Du, X. Yue, Z. Zhang, H. Zhang and G. Cui, *Part. Part. Syst. Charact.*, 2015, **32**, 1006–1011.

S17 L. Kong, C. Zhang, J. Wang, W. Qiao, L. Ling and D. Long, *ACS Nano*, 2015, **9**, 11200-11208.

S18 B. Li, F. Dai, Q. Xiao, L. Yang, J. Shen, C. Zhang and M. Cai, *Adv. Energy Mater.*, 2016, **6**, 201600802.

S19 P. Sennu, V. Aravindan, M. Ganesan, Y. –G. Lee and Y. –S. Lee, *ChemSusChem*, 2016, **9**, 849-854.

S20 F. Zhang, Y. Tang, H. Liu, H. Ji, C. Jiang, J. Zhang, X. Zhang and C. –S. Lee, *ACS Appl. Mater. Interfaces*, 2016, **8**, 4691-4699.

S21. A. Banerjee, K. K. Upadhyay, D. Puthusseri, V. Aravindan, S. Madhavi and S. Ogale, *Nanoscale*, 2014, **6**, 4387-4394.

S22. W. –H. Qu, F. Han, A. -H. Lu, C. Xing, M. Qiao and W. –C. Li, *J. Mater. Chem.*

A, 2014, **2**, 6549–6557.

S23. J. Come, M. Naguib, P. Rozier, M. W. Barsoum, Y. Gogotsi, P. -L. Taberna, M. Morcrette and P. Simon, *J. Electrochem. Soc.*, 2012, **159**, A1368-1373.

S24. H. Kim, M. -Y. Cho , M. -H. Kim, K. -Y. Park , H. Gwon , Y. Lee , K. C. Roh and K. Kang, *Adv. Energy Mater.*, 2013, **3**, 1500-1506.

S25. V. Khomenko, E. Raymundo-Piñero and F. Béguin, *J. Power Sources*, 2008, **177**, 643-651.

S26. P. Sennu, V. Aravindan, M. Ganesan, Y.-G. Lee, and Y. –S. Lee, *ChemSusChem*, 2016, **9**, 849-854.

S27. M. D. Stoller, S. Murali, N. Quarles, Y. Zhu, J. R. Potts, X. Zhu, H. –W. Ha and R. S. Ruoff, *Phys. Chem. Chem. Phys.*, 2012, **14**, 3388-3391.